Layer- and cell-type-specific suprathreshold stimulus representation in rat primary somatosensory cortex

C. P. J. de Kock, R. M. Bruno, H. Spors and B. Sakmann

Department of Cell Physiology, Max-Planck Institute for Medical Research, Jahnstrasse 29, D-69120 Heidelberg, Germany

Sensory stimuli are encoded differently across cortical layers and it is unknown how response characteristics relate to the morphological identity of responding cells. We therefore juxtasomally recorded action potential (AP) patterns from excitatory cells in layer (L) 2/3, L4, L5 and L6 of rat barrel cortex in response to a standard stimulus (e.g. repeated deflection of single whiskers in the caudal direction). Subsequent single-cell filling with biocytin allowed for *post hoc* identification of recorded cells. We report three major conclusions. First, sensory-evoked responses were layer- and cell-type-specific but always < 1 AP per stimulus, indicating low AP rates for the entire cortical column. Second, response latencies from L4, L5B and L6 were comparable and thus a whisker deflection is initially represented simultaneously in these layers. Finally, L5 thick-tufted cells dominated the cortical AP output following sensory stimulation, suggesting that these cells could direct sensory guided behaviours.

(Received 6 November 2006; accepted after revision 20 February 2007; first published online 22 February 2007)
Corresponding author C. P. J. de Kock: Department of Cell Physiology, Max-Planck Institute for Medical Research, Jahnstrasse 29, D-69120 Heidelberg, Germany. Email: christiaan.dekock@mpimf-heidelberg.mpg.de

Sensory cortices have a laminar architecture (Mountcastle, 1997), but the specific functions of each layer in information processing are largely unknown. To understand mechanistically the stream of electrical signals that sweeps through sensory cortices following a peripheral stimulus, both the subthreshold postsynaptic potential (PSP) and suprathreshold action potential (AP) response must be known. This is true for each layer but also for individual cells, since neuronal populations in a layer are not homogeneous. It is also essential to know the layer- and cell-type-specific AP response if one wants to understand the animal's behavioural response, since cells in the different layers project to specific target areas. The primary somatosensory barrel cortex of rodents provides a convenient system to elucidate sensory processing by neocortical areas because the individual facial whiskers are anatomically and functionally represented by discrete columns (Woolsey & Van der Loos, 1970; Simons, 1978).

Rodents when challenged with a behavioural task make responses on the basis of only a few whisker deflections (Carvell & Simons, 1995). We thus wanted to estimate the average AP response to a whisker deflection of the cells within a column and the relative contribution of the anatomically defined cell types at different times after stimulus onset. One view of cortical signalling is that the stream of sensory excitation begins with excitatory postsynaptic potentials in layer (L) 4, the principal recipient layer for thalamocortical afferents followed by AP activity in L4, which then spreads radially through the column to recruit L2/3, L5 and L6 (Carvell & Simons, 1988; Agmon & Connors, 1992; Armstrong-James *et al.* 1992; Moore & Nelson, 1998; Ahissar *et al.* 2000; Douglas & Martin, 2004). Layer 2/3 and L5 are considered the output layers and in turn excite other cortical areas, such as motor cortex, the brainstem nuclei that contribute to motor co-ordination and the subcortical nuclei involved in attention such as the striatum (Alloway *et al.* 1999; Jenkinson & Glickstein, 2000; Leergaard *et al.* 2000; Hoover *et al.* 2003; Hoffer *et al.* 2005). In addition, L5B and L6 project back to thalamus and could regulate thalamocortical interactions (Zhang & Deschenes, 1997; Killackey & Sherman, 2003).

Anatomical data suggest that layers other than L4 also receive direct thalamocortical input (Chmielowska *et al.* 1989; Lu & Lin, 1993). This is especially true for L5A (input from medial division of posterior nucleus; Koralek *et al.* 1988) and for L5B and L6 (input from ventroposterior medial nucleus of the thalamus; Chmielowska *et al.* 1989; Agmon *et al.* 1993). Thus, rather than a sequential activation of different layers, anatomical and physiological evidence suggests that parallel sensory processing in multiple layers could be possible (see also Mountcastle, 1957; Johnson & Alloway, 1995; Ahissar *et al.* 2001).

We previously determined the layer-specific subthreshold representation (PSP) of the same standardized

This paper has online supplemental material.

 DOI: 10.1113/jphysiol.2006.124321

stimulus (i.e. deflection of single whiskers) by *in vivo* whole-cell recordings of identified cells (Brecht & Sakmann, 2002*b*; Brecht *et al.* 2003; Manns *et al.* 2004). Here we characterize in a larger sample of identified cells the suprathreshold AP representation of single whisker deflections in different layers using juxtasomal recordings. We report that the AP output of a column is dominated by L5B thick-tufted pyramids.

Methods

Animal preparation

Urethane (1.6–1.7 g kg^{-1})-anaesthetized Wistar rats (55 animals of both sexes, postnatal day 25–30, 83.8 ± 11.1 g) were used. Depth of anaesthesia was checked by both foot and eyelid reflex and vibrissae movements. The animal's temperature was monitored with a rectal probe and maintained at 37°C by a thermostatically controlled heating pad. All experimental procedures were carried out according to the animal welfare guidelines of the Max-Planck Society. Experiments were performed on the primary somatosensory cortex (2.5 mm posterior and 5.5 mm lateral to Bregma) and ventroposterior medial nucleus of the thalamus (3.5 mm posterior and 3 mm lateral to Bregma), both in the left hemisphere. Whiskers contralateral to the recording site were trimmed to ∼5 mm. Single whiskers were subsequently deflected in random order at 3.3 deg in the caudal direction (ramp and hold, 8 ms rise time, onset–offset interval 200 ms, by a glass capillary attached to a piezoelectric bimorph (interstimulus time interval 2000 ms). We ruled out any substantial ringing of the bimorph by checking stimulator movement with a light circuit. Only onset responses were analysed.

Juxtasomal recordings

The column of interest was localized using intrinsic optical imaging (see Supplementary Fig. 1). We preferentially recorded from the D2 column (63 out of 77 recordings). A craniotomy of 0.5 mm × 0.5 mm was made covering the area of interest with the dura intact. *In vivo* juxtasomal recordings were made with 6–8 MΩ patch pipettes pulled from borosilicate filamented glass on a DMZ universal puller (Zeitz Instruments, Munich, Germany). Pipettes were filled with (mM): 135 NaCl, 5.4 KCl, 1.8 $CaCl_2$, 1 $MgCl_2$ and 5 Hepes, pH adjusted to 7.2 with NaOH, and 20 mg ml^{-1} biocytin was added. Bath solution contained 0.9% NaCl.

Single units were searched for using two methods. Initially we advanced the tip of the recording electrode in 2 μm steps every 2.5 s (0.4 Hz) while monitoring the occurrence of spontaneous APs (29 cells). In some experiments, the principal whisker was simultaneously deflected to increase AP activity. Action potentials would be recorded initially as negative-orientated waveforms but upon additional advance of electrode (generally 3–5 steps at 0.1 Hz) units were recorded as positive-orientated waveforms of 1–3 mV. In later experiments, the electrode resistance of the recording electrode was monitored while advancing in 2 μm steps (conventional method for whole-cell recordings). Using this method, unit isolation was independent of spiking frequency of cortical cells to ensure completely unbiased sampling (48 cells). Upon increase of electrode resistance, APs would generally already appear as negative-orientated waveforms. The electrode was then advanced stepwise at 0.1 Hz until positive AP waveforms were recorded with amplitudes of 1–3 mV (also additional 3–5 steps). Spiking properties (spontaneous and evoked APs) of cells isolated with either method were highly comparable (spontaneous activity, Mann–Whitney U test $P = 0.68$; evoked activity, Mann–Whitney U test $P = 0.61$), so data were pooled.

Recordings were made using an Axoclamp 2B amplifier (Axon instruments, Union City, CA, USA) in combination with a Lynx 8 amplifier, band filter settings 300 and 9000 Hz. Data were acquired using the Ntrode Virtual Instrument (R. Bruno, Heidelberg, Germany) for Labview (National Instruments, Austin, TX, USA). Typically, signal-to-noise ratios were of the order of 10:1 and recordings consisted of only a single positive-going unit. Spike data were sorted off-line using Mclust (A. David Redish, University of Minnesota, Minneapolis, MN, USA), primarily to check the quality of single-unit isolation. After physiological properties were measured, cells were filled with biocytin using current pulses (Pinault, 1996).

Histological procedures and reconstruction

Animals were transcardially perfused with 0.1 M phosphate buffered saline (pH 7.2), then 4% paraformaldehyde (PFA), and their brains were removed. Post fixation with 4% PFA was usually for 24 h. Tangential sections of 100 μm were made with a vibrotome. Cytochrome oxidase staining (Wong-Riley, 1979) was performed on slice 7–12 from PIA to visualize the barrel pattern characteristic of L4. The recorded cells were revealed with the chromogen 3,3′-diaminobenzidine tetrahydrochloride (DAB) using the avidin–biotin–peroxidase method (Horikawa & Armstrong, 1988). Slices were mounted on slides and embedded in mowiol (Clariant GmbH, Frankfurt am Main, Germany). Cells were reconstructed using Neurolucida software (Microbrightfield, Williston, VT, USA), using a ×100 oil objective.

Thalamic recordings

Cells located in ventroposterior medial nucleus of the thalamus (VPM) were identified physiologically by characteristic single (principal) whisker responses (tested

for eight directions; only caudal direction is shown here) and by their location relative to neighbouring thalamic nuclei, which have different response properties. Several thalamic recordings were made on the same electrode track, but not all cells were filled with biocytin. The thalamus was cut in coronal sections and stained for cytochrome oxidase and biocytin. The identity of cells in VPM was confirmed *post hoc* by comparing VPM staining, electrode tracks, filled cell locations and recording depth.

Data analysis

Spontaneous activity was calculated during the 100 ms prestimulus windows averaged for all trials and all whiskers tested. The evoked response was quantified in the 0–100 ms after the stimulus, and average spontaneous activity was subtracted. To determine the latency to response onset, we compared spontaneous AP firing during the prestimulus period with APs in the 0–100 ms after the stimulus. Spontaneous AP firing was modelled as a Poisson distribution, and latency was defined as the first 1 ms bin for which AP counts significantly exceeded prestimulus levels ($P < 0.01$). In the absence of prestimulus APs, the first AP in the post-stimulus period was used to determine onset latency. The coefficient of variation was calculated by counting all APs in 0–100 ms after the stimulus on a trial-to-trial basis without correction of spontaneous activity. All values are presented as means ± S.D. In boxplots, the grey box represents the 25th–75th percentile, the long vertical lines the 10th–90th percentiles, and the dark horizontal line the median.

Statistical analysis

Graphpad Instat 3 (San Diego, CA, USA) was used for statistical analysis. Generally, data were not normally distributed. Therefore, we used the non-parametric ANOVA (Kruskal–Wallis test) for comparison of all cell types, followed by Dunn's *post hoc* test for comparison of two individual cell classifications. For comparison of receptive field size (Fig. 7), we used repeated measures ANOVA with the Bonferroni correction. The (non-parametric) Mann–Whitney *U* test was used for comparison of correlation coefficient between and across cell types (Fig. 5*D* inset). Significance level was set at $P < 0.05$.

Results

Morphological classification of recorded neurones

The cortical column consists of multiple cell layers which in addition contain specific cell types (Mountcastle, 1997). We recorded from cells preferentially located in the D2 column (see Supplementary Fig. 1; 63 D2, 2 D1, 10 D3 and 2 D4 cells). Action potential responses were recorded in the juxtasomal configuration, and cells were subsequently filled with biocytin for morphological identification (Pinault, 1996). Recovered neurones were classified according to their location with respect to the cytochrome oxidase dense area, characteristic of layer 4 (L4). Septa-related cells were excluded from the analyses because they are part of different anatomical and functional networks (Kim & Ebner, 1999). Interneurones were excluded owing to the small sample size.

We categorized cells as L2/3 cells when their cell body was located in supragranular layers (Fig. 1*A*, $n = 15$; see also Supplementary Fig. 2). The descending axon was traced into L4 to confirm that the cell was part of the barrel-related column and not the septum.

Cells that were located in the cytochrome oxidase dense volume were categorized as L4 cells. L4 cells can be further subdivided into spiny stellates and (star) pyramids based on the absence (stellate) or presence (pyramid) of an apical dendrite and on symmetry of basal dendrites (Staiger *et al.* 2004). Out of the 15 cells recorded, five cells clearly lacked an apical dendrite and were therefore classified as spiny stellates. An apical dendrite could be easily identified in seven cells recorded, which were classified as pyramidal neurones (of which 3 were star pyramids). We also recorded from cells with morphology that could be part of either class ($n = 3$). No obvious differences in response properties were found between spiny stellates and (star) pyramids (number of APs per stimulus and latency to first AP, unpaired Students *t* test, $P = 0.9$ and $P = 0.4$, respectively) and therefore data were pooled (see also Brecht & Sakmann, 2002*b*).

In L5, several cellular classifications exist, depending on experimental design (Markram, 1997; Schubert *et al.* 2001, 2006; Manns *et al.* 2004). We used morphological parameters to classify L5 cells. First, we measured the diameter of the apical dendrite and the maximal horizontal diameter of the cell body (Fig. 1*B*). This relationship suggested two distinct populations, most probably representing medium-sized pyramidal neurones in L5A and large pyramidal neurones in L5B (Wise & Jones, 1977). The initial clustering was confirmed by measuring the length of apical tuft and oblique dendrites compared with the total length of the basal dendrites (Fig. 1*C*). In the first cluster, the total length of basal dendrites always exceeded the total length of the apical dendrite, suggesting a simple apical tuft. In contrast, the total length of the apical tuft in the second cluster always exceeded the total length of basal dendrites, suggesting extensive branching of the apical tuft. Accordingly, cells were categorized either as L5 slender-tufted cells or L5 thick-tufted cells ($n = 16$ for both cell types). Statistical analysis of the individual morphological properties (unpaired Student's *t* test) revealed that the diameter of the cell body, diameter

of apical dendrite and total length of apical dendrite were significantly different for L5 slender-tufted and L5 thick-tufted cells ($P < 0.01$). The difference in total length of basal dendrites was at trend level ($P = 0.08$) but the ratio between total length of apical and basal dendrites (Fig. 1*C*) was again highly significant (Mann–Whitney *U* test, $P < 0.01$).

We subsequently analysed the vertical distance between the cytochrome oxidase dense volume and the cell bodies of L5 slender-tufted cells to determine whether they were located in L5A or L5B. In 13 out of 16 cells, the cell body was found within three slices distance from L4 (i.e. within ~300 μm). Since the thickness of L5A in our animals is about 300 μm (Manns *et al.* 2004), this suggests that we predominantly recorded from L5 slender-tufted cells located in L5A.

Layer 6 cells were identified based on their short apical dendrite that never extended beyond the granular layer ($n = 15$). Next, we subclassified L6 cells as corticothalamic, corticocortical or local circuit cells. Corticothalamic cells can be identified with respect to their basal dendrites that are arranged in a skirt-like order typical of pyramidal

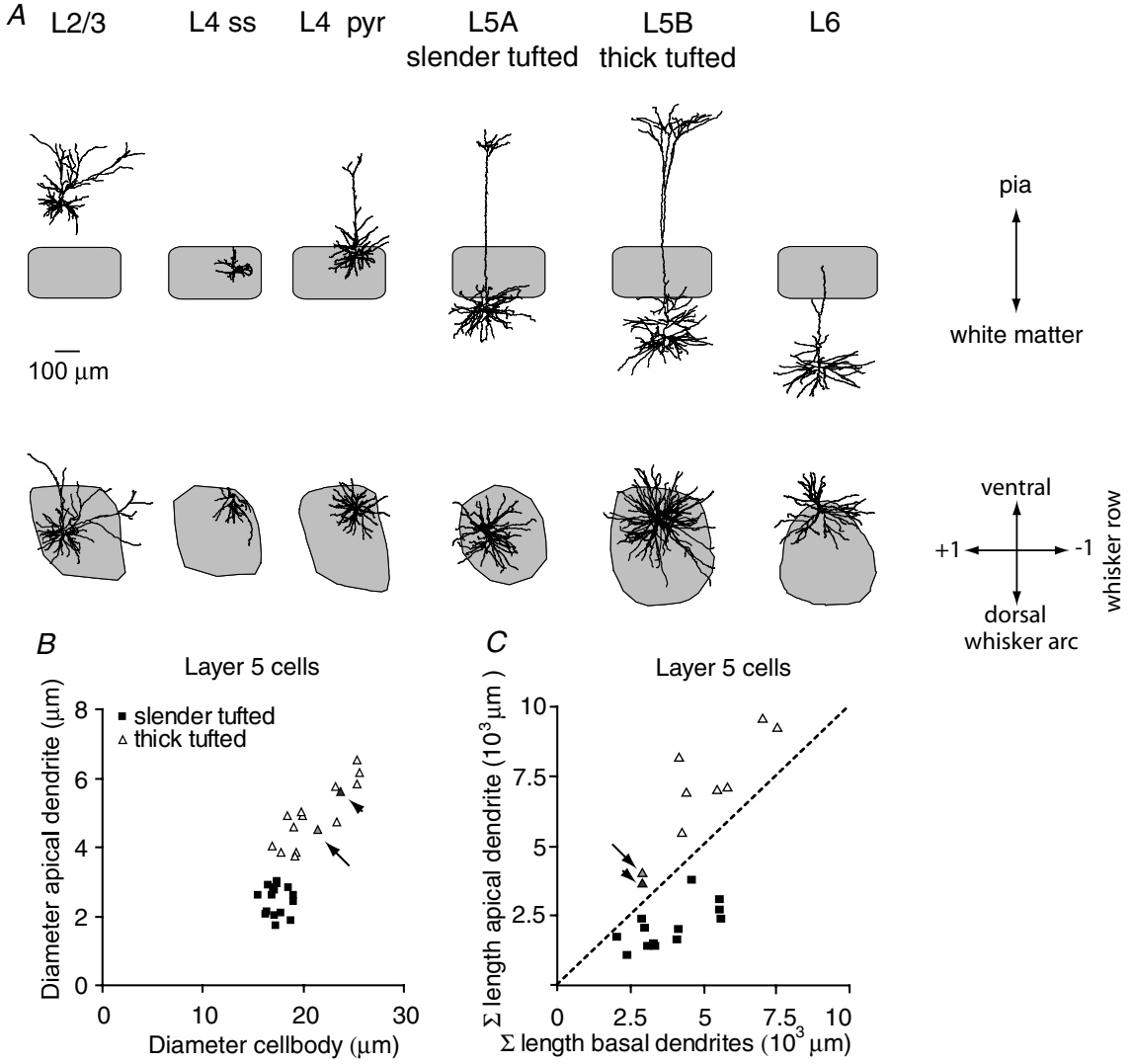

Figure 1. Classification of barrel-related cells
A, reconstructions of representative examples in coronal (top) and tangential view (bottom). The grey shape shows the contour of the D2 column, representing the cytochrome oxidase dense area in L4. *B*, diameter of apical dendrites of L5 cells compared with cell body diameter suggests two populations of L5 cells (slender-tufted, average diameter of soma 17.4 ± 1.0 μm and diameter of apical dendrite 2.5 ± 0.4 μm; thick-tufted, diameter of soma 21.1 ± 3.0 μm and diameter of apical dendrite 4.9 ± 0.9 μm). *C*, for thick-tufted cells, the total length (Σ) of the apical dendrite (apical tuft and oblique dendrites) always exceeds the total length of the basal dendrites. In L5 slender-tufted cells, this relationship is reversed. Note that L5 cells may have intermediate values (arrow and arrowhead). These cells were categorized as thick-tufted cells, based on diameter of the apical dendrite and appearance of apical tuft.

cells, and corticocortical cells on their star-like appearance owing to more radiating basal dendrites, whereas local circuit cells have characteristic smooth-beaded dendrites (Zhang & Deschenes, 1997). As a result, we identified eight cells as corticothalamic and five cells as corticocortical cells ($n = 2$ with intermediate morphology). No obvious differences in responses were found among possible subclassifications of L6 cells (see below).

Action potentials in response to whisker deflection

It is established that in barrel cortex neurones are direction selective and AP responses to whisker deflections can be higher in a preferred direction (Bruno *et al.* 2003). In contrast, rodents respond to the sensory input from only one or two whisker deflections when challenged with a behavioural task (Carvell & Simons, 1995) and single whiskers are sufficient for many sensory-guided behaviours (Hutson & Masterton, 1986). Here we studied how a single standard sensory stimulus, that is a single whisker deflection in the caudal direction, is represented throughout the cortical column by different cell types and layers. In addition, we present data from ventro-posterior medial nucleus (VPM) recordings to directly compare sensory representation in thalamus and the cortical column (Figs 3*C*–*E* and 4).

We quantified spontaneous AP rates and the averaged evoked AP responses following repeated deflection of the principal whisker (PW, 20 or 50 trials, caudal 3.3 deg deflection) using only identified cells (as illustrated by the representative examples of cortical recordings in Fig. 2; VPM data not shown). Most trials exhibited a change in the local field potential but not necessarily APs (Fig. 2*A* and *B*). Layer 2/3 cells responded with an AP only in rare cases, whereas L4 cells showed a more consistent AP response. Layer 5 slender-tufted cells were characterized by low evoked AP responses and longer latency to response onset, whereas L5 thick-tufted cells mostly responded with short latencies and higher AP responses. In L6, evoked responses were variable, with cells characterized by high AP responses with short latencies in addition to cells with low evoked AP responses and long latencies. Spontaneous spiking rates were significantly different depending on the cell type (Fig. 3*A*–*C*): L2/3 0.32 ± 0.49 Hz; L4 0.58 ± 0.36 Hz; L5 slender-tufted 1.08 ± 0.38 Hz; L5 thick-tufted 3.65 ± 1.32 Hz; L6 0.47 ± 0.46 Hz; Kruskal–Wallis test, $P < 0.0001$).

The average evoked AP response after correction for spontaneous activity (see Methods) for L2/3 cells was 0.11 ± 0.14 APs during the 100 ms post-stimulus window (Fig. 3*A*, *B* and *D*), with a trend towards higher response amplitudes for cells located deeper in

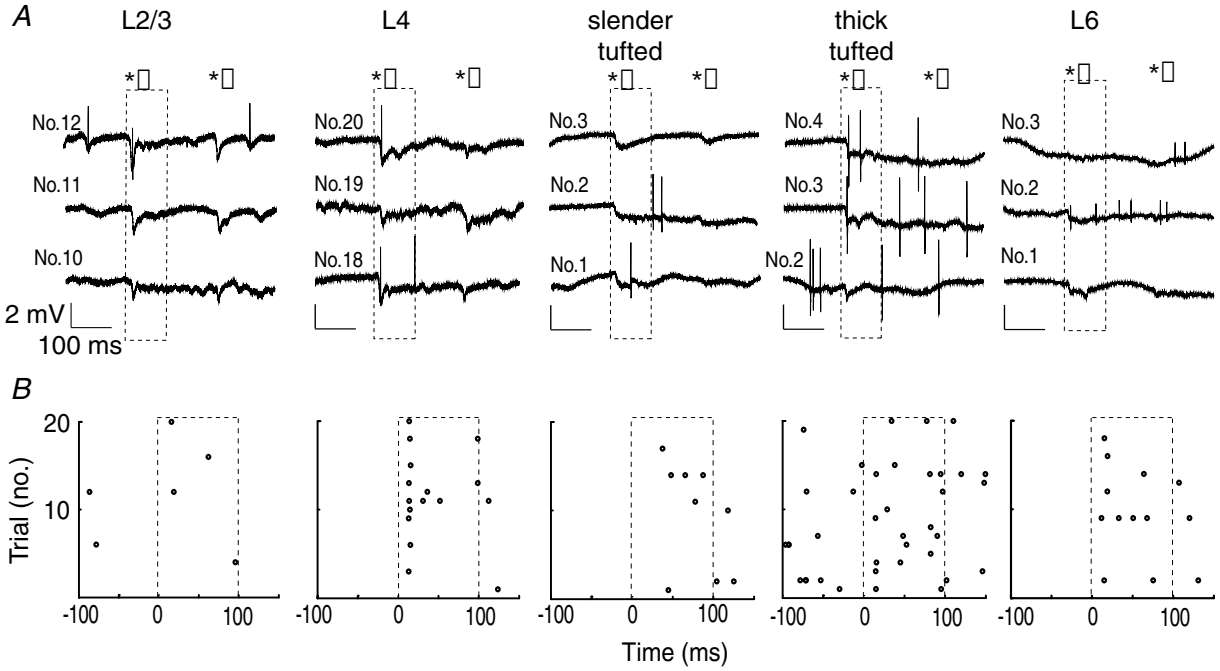

Figure 2. Cortical APs in response to principal whisker deflection
A, 3 consecutive (unfiltered) single trial examples of juxtasomal recordings in different layers of the D2 column of barrel cortex. The asterisks illustrate the onset and offset of whisker movement, whereas the dashed box represents the first 100 ms after stimulus onset used to quantify evoked APs. *B*, raster plots showing all trials for single example cells shown in *A*. Note that AP responses are layer-specific and that the slender-tufted cell has the longest latency to spiking.

L2/3 (Supplementary Fig. 3). Layer 4 cells showed a threefold higher evoked AP response (0.41 ± 0.41 APs per stimulus). Evidently, the number of APs per stimulus was well below one, indicating that many failures occurred (Fig. 3*B*). The response of L5 slender-tufted cells was characterized by a low number of APs per deflection (0.15 ± 0.35 APs per stimulus), whereas L5 thick-tufted cells showed the most pronounced increase in spiking activity (0.64 ± 0.47 APs per stimulus). Layer 6 cells had intermediate evoked responses (0.31 ± 0.35 APs per stimulus). Cells with relatively high response amplitudes were primarily located in the upper region of L6, where thalamic fibres arborize extensively (Agmon *et al.* 1993), whereas non-responding cells were mainly found in lower parts of L6 (Supplementary Fig. 3).

As mentioned above, we recorded from eight cortico-thalamic and five corticocortical cells ($n = 2$ with intermediate morphology) but found no significant differences

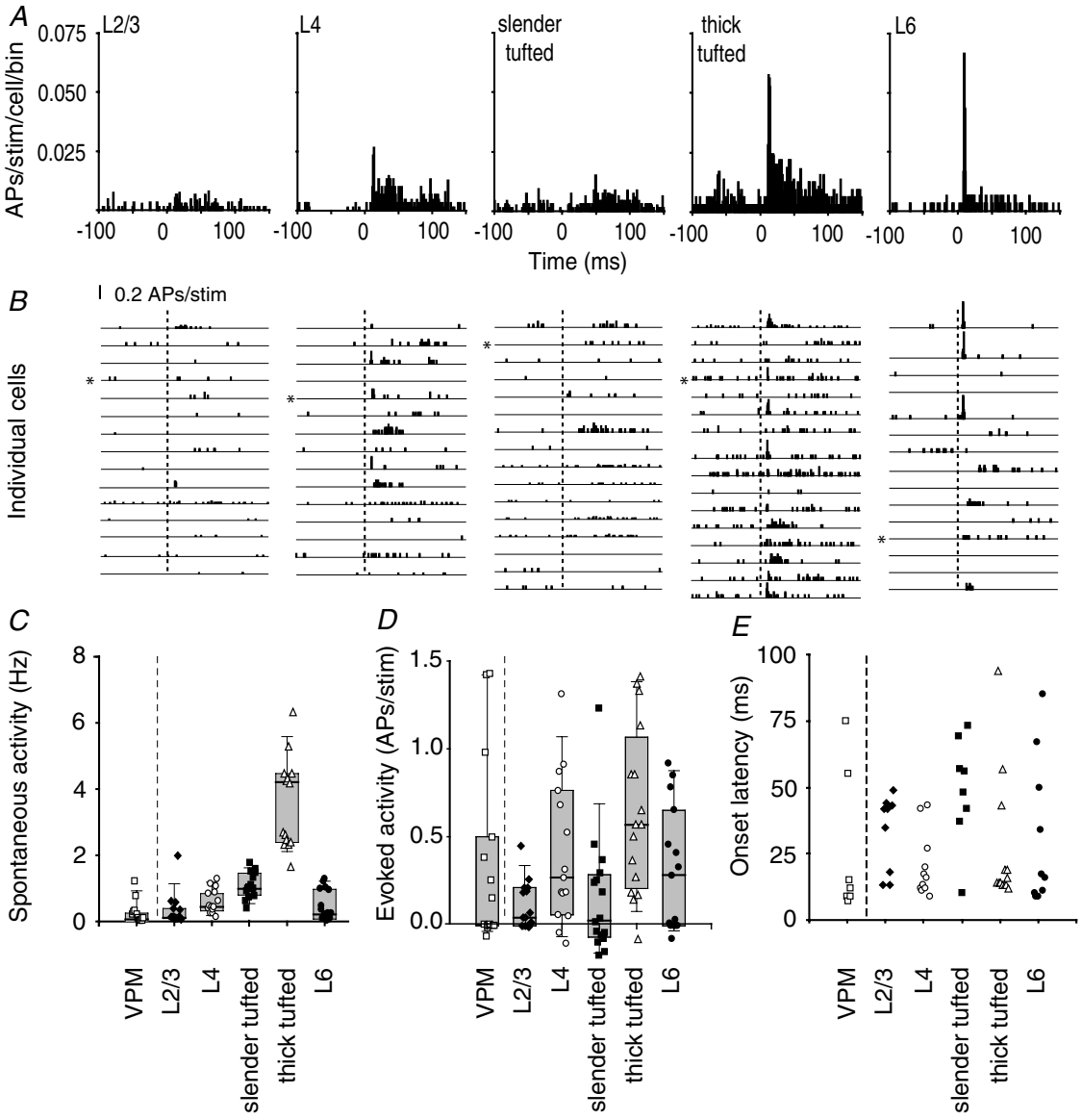

Figure 3. Layer- and cell-type-specific AP responses after principal whisker deflection
A, average peristimulus time histograms (PSTHs) to illustrate the response in time after deflection of the principal whisker (1 ms bins, $n = 15$ cells for L2/3, L4 and L6; $n = 16$ for both L5 slender- and thick-tufted cells). *B*, individual PSTHs for all experiments from different cell types. Asterisks indicate experiments shown in Fig. 2. Dashed lines indicate onset of principal whisker stimulation. *C*, spontaneous activity for different cell types. Recordings were also made from the ventroposterior medial nucleus of the thalamus (VPM, $n = 15$, 0.21 ± 0.33 Hz). *D*, number of evoked APs after a whisker deflection (0–100 ms after stimulus, after subtraction of spontaneous activity). Negative values indicate evoked AP responses below spontaneous values. Evoked activity in VPM was 0.35 ± 0.53 APs per stimulus. *E*, onset latency for individual experiments that showed an evoked response.

between evoked response amplitudes and latency for these subclassifications (Mann–Whitney U test, $P = 0.13$ and $P = 0.11$, respectively). We hypothesize that rather than dendritic morphology, the soma location and possibly direct thalamic input in upper L6 may determine the response characteristics (also see Supplementary Fig. 3).

It has been shown that in particular, L5 thick-tufted cells are capable of firing in bursts (Chagnac-Amitai *et al.* 1990; Mason & Larkman, 1990; Schubert *et al.* 2001). We therefore analysed whether in these cells, the fraction of high-frequency bursts (> 100 Hz) was increased as a possible explanation for the relatively high spontaneous and evoked activity. We found that the occurrence of spontaneous high-frequency bursts in general was very limited (∼11%) and was not different for L5 thick-tufted cells compared with other layers (Kruskal–Wallis with Dunn's *post hoc* test, n.s., data not shown). For the evoked activity, the fraction of high-frequency bursts again was very limited (∼10%) and only significantly higher for L5 thick-tufted cells compared with L2/3 cells (Kruskal–Wallis with Dunn's *post hoc* test, n.s., data not shown) but not for other layers (n.s., data not shown). We conclude that spontaneous firing rates and sensory responses in barrel cortex are dominated by single APs.

On the basis of the AP responses of the cell types present in each layer, one can infer an upper percentage limit of active cells per stimulus (e.g. L2/3 cells, 11%) assuming homogeneous populations. In all layers, a subset of cells lacked a sensory-evoked response when the PW was deflected. This could result from stimulation in the non-preferred direction (Bruno *et al.* 2003) and/or a characteristic of a columnar network in which only a small percentage of cells is activated upon a sensory stimulus.

With respect to simultaneous or sequential AP representation of a sensory stimulus in cortical layers, controversial results have been reported. This is most likely caused by a lack of knowledge about the identity of responding cells. To determine the laminar pattern of electrical activity after a sensory stimulus, we measured the latency to the first AP for individual identified cells (Methods). In L2/3 and L5 slender-tufted cells, evoked AP responses were very low, and latency estimates would be based on single APs, making their interpretation ambiguous. In contrast, in L4 spiny cells, L5 thick-tufted cells and L6 cells, the responses were sufficient to derive latency distributions.

We found very short onset latencies (9–13 ms) in a subset of L4 cells, in L5 thick-tufted cells and in L6 cells (Fig. 3*E* and, at higher time resolution, in Fig. 4*C*). The median onset latencies of L4 cells, L5 thick-tufted cells, and L6 cells (16, 14 and 16.5 ms, respectively) were not significantly different (Kruskal–Wallis test, $P = 0.8147$, $n = 10$–13 per group). This does not necessarily imply that average AP latencies are the same, but at this point we conclude that latency distributions overlap. The absence of a significant difference might be result from our small sample size. To estimate the power of statistical testing for difference in l'atency, we calculated the power of unpaired Students t test using different effect sizes (in ms). To achieve normally distributed data a log transform was applied. As a result, the data were close to normally distributed. For all comparisons between cell types, the probability of a type II error was lower than 0.01 for an effect size ≥ 3 ms, which indicates that average onset latencies of stimulus representation are very similar for L4 cells, L5 thick-tufted cells and L6 cells. This is also clear from the population peristimulus time histograms (PSTHs) for these cell types when shown at higher time resolution (Fig. 4*A*), which shows that the average firing rates increased in L4, L6 and L5 thick-tufted cells almost simultaneously (see also Fig. 4*C*).

To detect possible differences in shape of the population PSTHs, cumulative histogram distributions were calculated. At each post-stimulus time point, the sum of all APs was calculated in that particular post-stimulus time window and represented as a percentage of the total number of APs in the total (e.g. 0–20 ms) post-stimulus window (Fig. 4*B*). This also shows that after whisker deflection, L6 cells are activated first, closely followed by L4 and L5 thick-tufted cells, and that the shapes of the population PSTHs are cell-type-specific. It is unlikely that initial activity in L5 thick-tufted cells and L6 depend on intracortical spread of activity originating from L4. Rather, parallel activation of L4, L5 thick-tufted cells and L6 could result from simultaneous input by the same thalamic inputs (Chmielowska *et al.* 1989; Agmon *et al.* 1993; Ahissar *et al.* 2001).

To find out whether there is a relationship between spontaneous activity, evoked response and latency of cortical cells, we correlated these parameters for all cells recorded. We did not find a correlation between evoked activity and latency within individual cell classification (P values > 0.16). On the population level, however, latency was inversely correlated with spontaneous activity ($P = 0.02$, data not shown). This suggests that cells with high spontaneous activity might have membrane potentials close to AP threshold, which result in shorter response latencies after a sensory stimulus. In support of this argument, we also found a positive correlation on the population level between spontaneous activity and evoked activity ($P < 0.01$, data not shown).

Laminar comparison of trial-to-trial variability of evoked AP responses

Cortical networks are known for their variability of evoked sensory responses both from trial to trial and from cell to cell (Arieli *et al.* 1996; Amarasingham *et al.* 2006). However, it is unknown how response variability relates to particular cell types. Here we first examined

the trial-to-trial variability, which is thought to represent the capability of neurones to reliably transmit signals, by calculating the coefficient of variation (c.v.; standard deviation/mean). The analysis was also made with records of cells from the VPM to compare the reliability of thalamic and cortical sensory-evoked responses. The c.v. analysis was first made for data uncorrected for spontaneous APs. The range of c.v. was comparable between VPM and all cortical layers (Fig. 5*A*) and declined with increased mean responses (Fig. 5*B*). Values of c.v. in VPM, L4, L5 thick-tufted and L6 cells tended towards lower values, indicating more consistent stimulus representation during repeated stimulation (Fig. 5*A*). To verify that spontaneous APs did not influence the c.v. estimates, we calculated

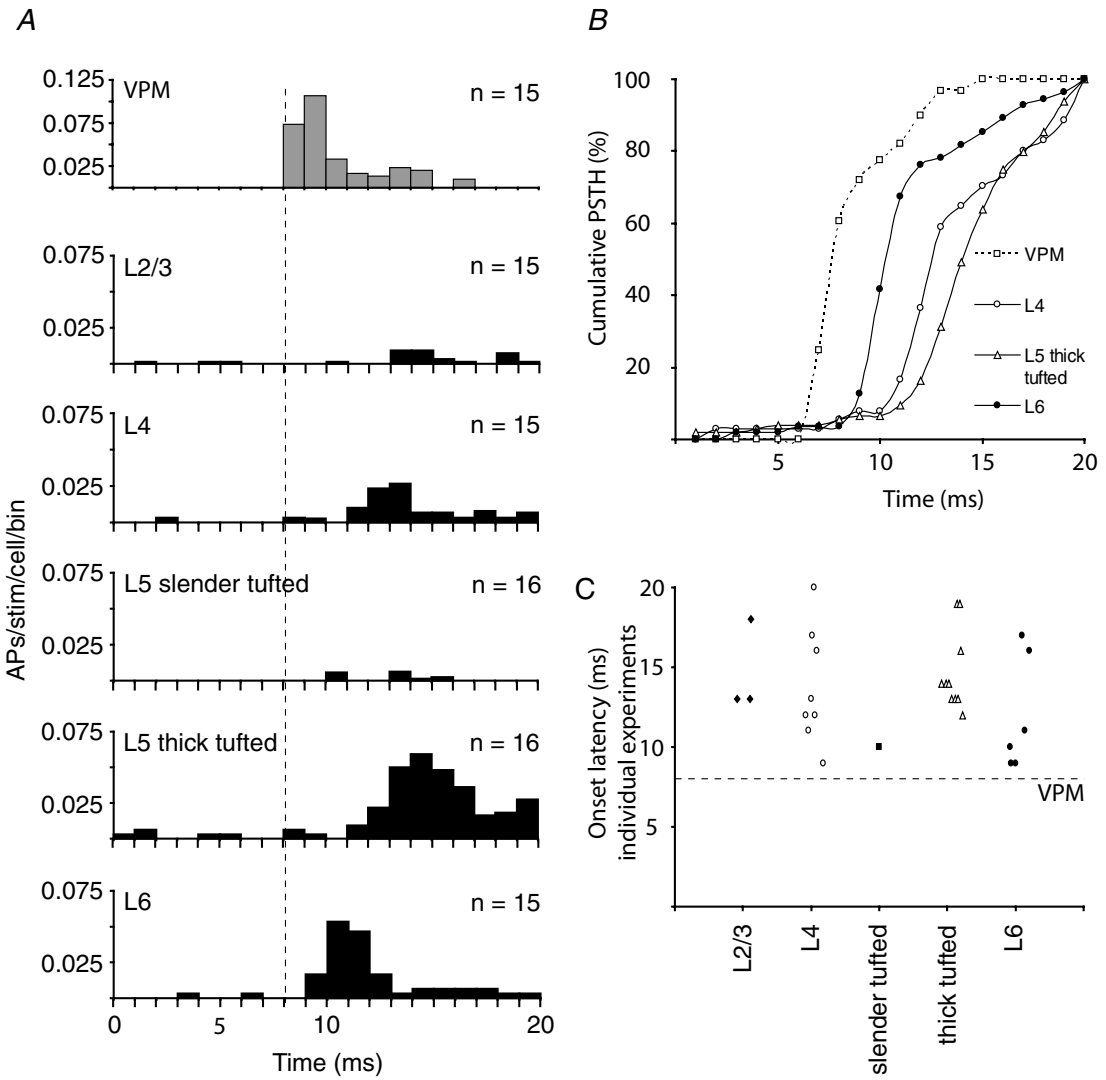

Figure 4. Near-simultaneous stimulus representation in multiple cell types
A, average PSTHs illustrating the response in time after deflection of the principal whisker. Note that the upper panel represents data from VPM recordings. Data from cortical recordings are analogous to Fig. 3*A* but at higher time resolution (only 0–20 ms post-stimulus time window is shown). The vertical line indicates the onset of VPM activity at 8.1 ms post-stimulus (Brecht & Sakmann, 2002*a*). *B*, cumulative distribution of APs occurring within the first 20 ms after the onset of the principal whisker deflection (data from *A*). The steepest part of the curves indicates the time window when the majority of the APs occurred within the first 20 ms. The *x*-axis is the time in milliseconds relative to the onset of the principal whisker deflection; *y*-axis is the proportion of APs up to the corresponding time point after the stimulus (e.g. 100% at 20 ms). Distribution and amplitude of AP responses were significantly different for L4, L5 thick-tufted cells and L6 cells (Kolmogorov–Smirnov test, $P < 0.01$ for all comparisons). *C*, onset latency for individual experiments that showed an evoked response. Data are analogous to Fig. 3*E* but only the 0–20 ms onset latency values are shown.

c.v. values both on data in which spontaneous activity was subtracted and on total AP responses with a shorter time window (50 ms; contribution of spontaneous APs is limited). In both additional analyses, VPM, L4, L5 thick-tufted cells and L6 still had lower c.v. values compared with L2/3 and L5 slender-tufted cells (data not shown). We conclude that those cortical cells that receive direct VPM input have reliable whisker-evoked responses relative to cells that are activated via other or additional pathways [intracortical and medical division of posterior nucleus (POm) inputs for L2/3 and L5 slender-tufted cells].

To quantify the similarity of evoked responses between individual cells (0–100 ms post-stimulus window), we calculated Pearson correlation coefficients for all cell-to-cell combinations using PSTHs from individual cells at 1 ms resolution (Fig. 5*C*). A correlation (or similarity value) of one means that two PSTHs have the same shape (i.e. they could be identical or they could simply be shifted with respect to baseline frequency. Here the mean of each PSTH is being subtracted and so spontaneous activity is corrected for. A correlation value of zero means no apparent correlation between the

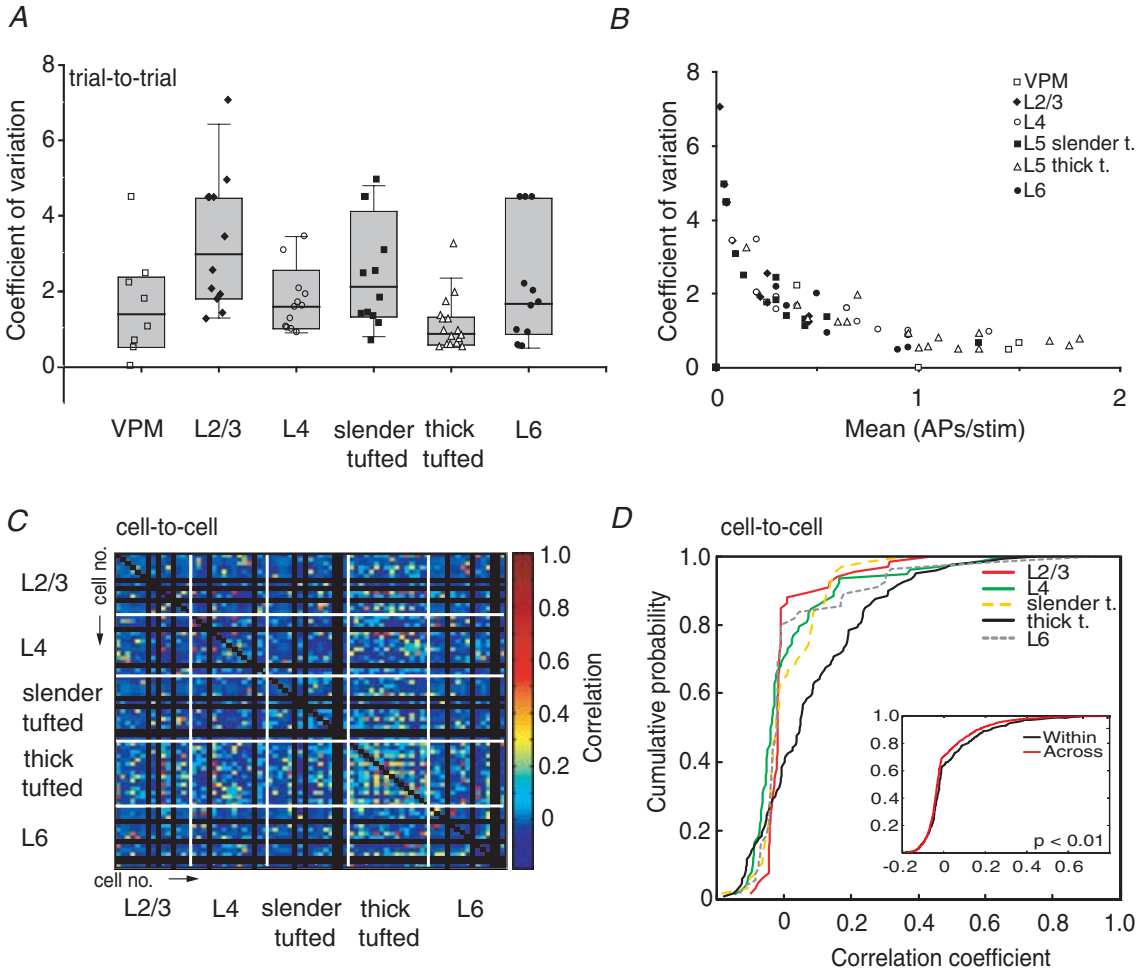

Figure 5. Laminar comparison of AP response variability
A, distribution of trial-to-trial response consistency for individual experiments. Higher values indicate higher variability of principal whisker-evoked responses. *B*, coefficient of variation as a function of mean response amplitude across cell types. *C*, correlation of evoked responses (e.g. PSTHs) between cells. The *x*- and *y*-axes both represent individual experiments. Each pixel corresponds to the correlation value between evoked response patterns during the 0–100 ms post-stimulus time. The correlation coefficient is colour coded. Note that highest correlation values are obtained when comparing L5 thick-tufted cells with other L5 thick-tufted cells, indicating that cell-to-cell variability is lowest. *D*, correlation values from *C* were plotted in a cumulative histogram for all cell types. Note that L5 thick-tufted cells have the highest correlation values. Inset shows cumulative histogram for correlation values from comparison within each cell type (black line) or across cell types (red line). Correlation values for within comparison were significantly higher compared with correlation values across (Mann–Whitney *U* test, $P < 0.01$), indicating that within cell types, variability is lower compared with variability between cell types.

two PSTHs and a correlation coefficient of minus one indicates 'anticorrelation', meaning that the cells discharge at complementarily different times. We found highest similarity values if we compared whisker-evoked responses from L5 thick-tufted cells with other L5 thick-tufted cells. Other cell types had lower values, indicating higher cell-to-cell variability. The cumulative histogram obtained from the similarity analysis also indicated that L5 thick-tufted cells had the highest values (Fig. 5*D*). In summary, L5 thick-tufted cells have the lowest trial-to-trial variability and cell-to-cell variability.

Dynamic receptive fields throughout cortical column after whisker deflection

In previous studies, it was shown that in L2/3, L4 and L5B the subthreshold receptive field (PSP-RF) structure emerged at early time points (~15 ms) and then collapsed in a layer-specific way ranging from 80 to 160 ms after whisker deflection (Brecht & Sakmann, 2002*b*; Brecht *et al.* 2003; Manns *et al.* 2004). Only L5A cells had later onset latency (~40 ms), but also collapsed in the following 80 ms. To compare previous PSP-RFs data with the present AP responses, we constructed population receptive fields (AP-RFs) for each layer using comparable time windows (Fig. 6). We found that the peak of the RF was highest for L2/3, L4, L5 thick-tufted and L6 cells already 10–20 ms after whisker stimulation and collapsed after 50 ms. The L5 slender-tufted cells exhibited their peak response at longer latencies, but also the RF was collapsed after another 50 ms. In addition, AP-RFs are almost completely restricted to PW responses in L2/3, L4, L5 slender-tufted and L6 cells. Clear surround whisker (SuW) responses were, however, observed for L5 thick-tufted cells. Thus the dynamics of the AP-RFs match PSP-RFs for L4 and L5A slender-tufted pyramids, but the AP-RFs develop and collapse faster in L2/3 and L5B thick-tufted pyramids.

The RF for the 100 ms post-stimulus time window was constructed by measuring AP responses after deflection of SuWs. For all cell types measured, on average the principal whisker evoked the largest response (Figs 6 and 7*A* and *B*). The RFs of L2/3 cells were relatively sharply tuned, with only small responses after first order SuW deflection (0.04 ± 0.02 APs per stimulus, $32.6 \pm 20.6\%$

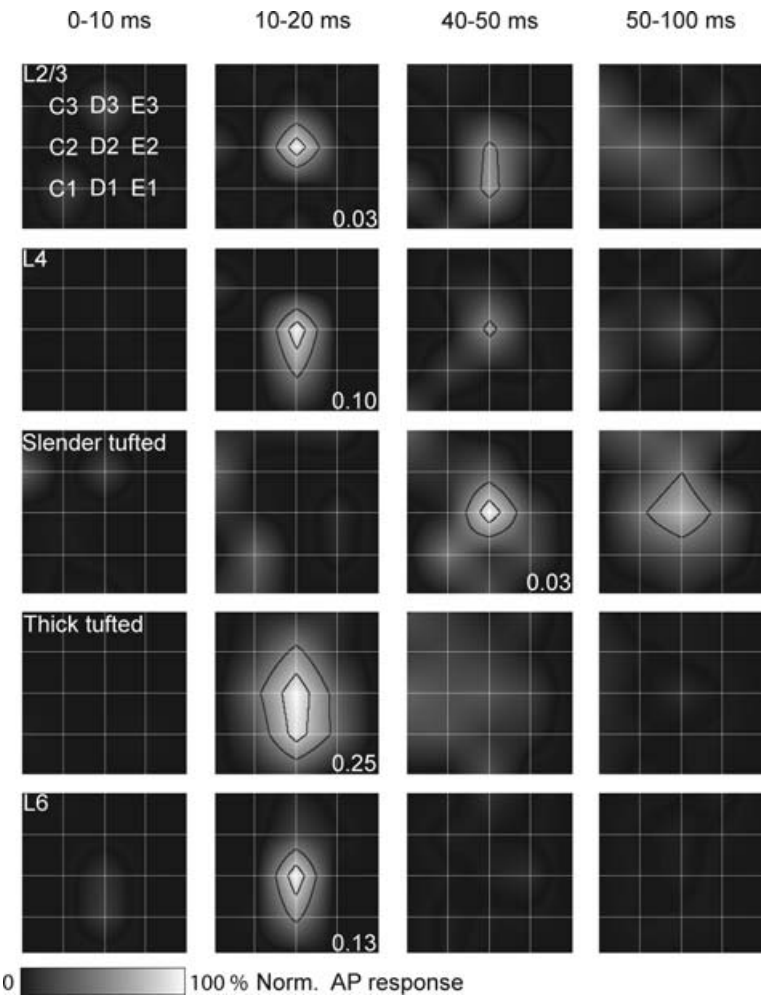

Figure 6. Layer-specific dynamics of suprathreshold RF structure
The grid of white lines indicates the barrel field, with the intersection representing the centre of the barrel with the principal whisker aligned in the middle. Surround whisker responses were normalized to the principal whisker response. The black lines delineate the areas equal to 80 (inner contour) and 50% (outer contour) of the maximal principal whisker response. Responses were normalized to the peak response within each layer. The numbers indicate average evoked response (APs per cell per stimulus) for the time window in which maximal firing was observed.

of PW response, Fig. 7*B*). The L4 cells responded predominantly to PW deflection, with a SuW response of only 0.06 ± 0.06 APs per stimulus ($15.6 \pm 14.2\%$). Average RF size of L5 slender-tufted cells was comparable to L2/3 cells ($31.3 \pm 25.3\%$, 0.05 ± 0.03 APs per stimulus). In contrast, L5 thick-tufted cells showed significantly higher responses after SuW deflection (0.39 ± 0.12 APs per stimulus, repeated measures ANOVA with Bonferroni correction, $P < 0.05$ for all cell types). After normalization to PW response, L5 thick-tufted cells still showed a significantly broader RF ($60.1 \pm 19.0\%$, repeated measures ANOVA with Bonferroni correction, $P < 0.05$ for all cell types). The RF of L6 was characterized by a dominant PW response (0.31 ± 0.35 APs per stimulus) and weak SuW responses (0.08 ± 0.06 APs per stimulus, $26.9 \pm 20.4\%$).

Sensory-guided behaviour most probably depends not only on activity in the cortical column that corresponds to the PW but also on activity in surrounding barrel columns. We therefore estimated the average output of every cell by summing the number of APs per stimulus for the PW and all first order SuWs. Then, L5 thick-tufted cells have significantly higher output compared with all other cell types (Fig. 7*C*, one-way ANOVA, Bonferroni correction, $P < 0.001$ for all cell types). To conclude, L5 thick-tufted cells have the broadest RF compared with other cell types, responding with APs to deflection of whiskers surrounding the PW.

Action potentials generated in a column

The total number of APs emitted from the cortical column can now be estimated when we account for the number of cells present in each layer. In our tangential slices, the area of the D2 column was measured as $\sim$120 000 μm^2. The thickness of the cortical layers was taken from previous reports (Brecht & Sakmann, 2002*b*; Brecht *et al.* 2003; Manns *et al.* 2004). Calculated volumes were subsequently multiplied by known cell densities for the individual layers, corrected for inhibitory cells (Beaulieu, 1993). We thus estimated 3200 L2/3, 2050 L4, 1100 L5A, 1050 L5B and 1200 L6 excitatory cells (Supplementary Table 1). For VPM, we used 200 cells (Varga *et al.* 2002). Since there does not seem to be an overall bias of angular preferences in primary somatosensory (barrel) cortex (Bruno *et al.* 2003; Bruno & Sakmann, 2006), the average response amplitude of our sample will correctly estimate the average

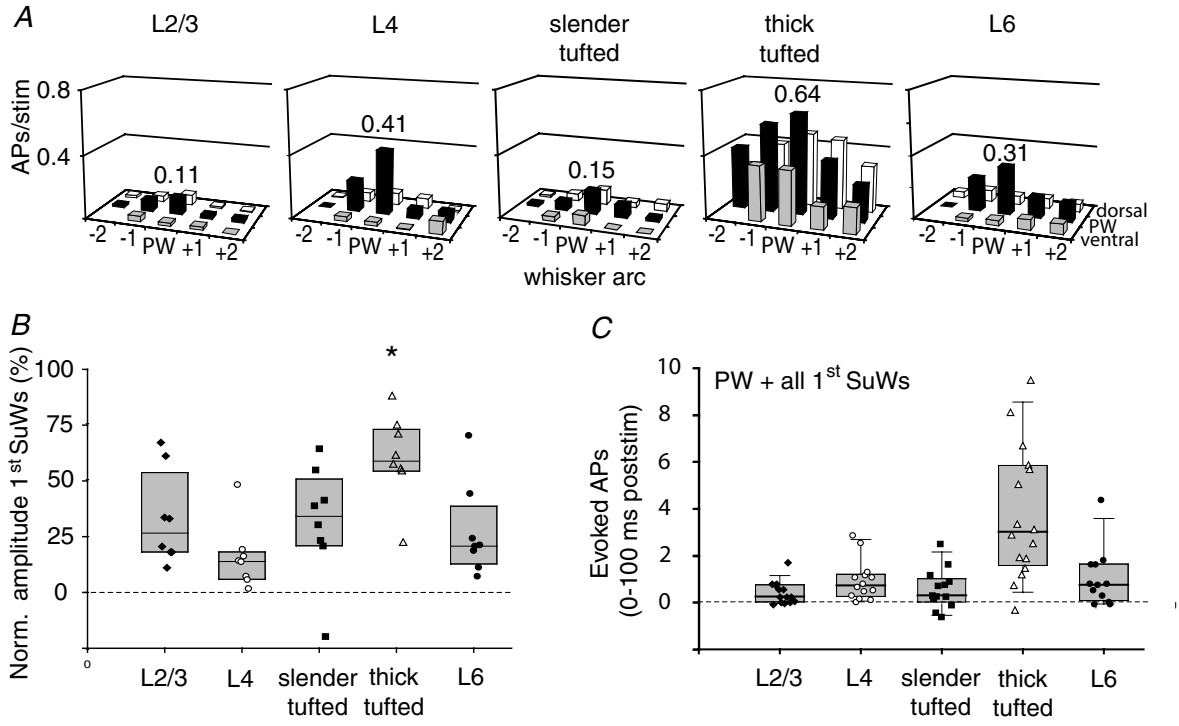

Figure 7. The output of a cortical column is dominated by L5 thick-tufted cells
A, receptive fields (RFs) for the different cell types illustrate evoked AP activity after deflection of principal and surround whiskers in the 0–100 ms post-stimulus period, centred on their principal whisker according to the anatomical location (63 D2, 2 D1, 10 D3 and 2 D4 cells). *B*, responses of surround whiskers were normalized to principal whisker response for each layer. Note that the RF of L5 thick-tufted cells is significantly broader than the RF of all other cell types. *C*, total number of evoked APs summed for the principal whisker and all first order surround whiskers in the 0–100 ms post-stimulus time window. Only experiments in which all 8 surround whiskers were measured were included.

response across all cells, despite their individual tuning preferences. Therefore, the cell numbers were multiplied by the average number of APs in response to a deflection to generate the total number of APs per cell layer during specific time windows after sensory stimulation (Fig. 8*A* and *B*, grey values normalized to maximum; note that the last two intervals were corrected for a larger time window). Under these conditions, clearly the number of APs emitted at any time, spontaneously (Fig. 8*A*) and after whisker deflection (Fig. 8*B*), is very different depending on layer and cell type and by far exceeds the number of APs that are fired in VPM (see also Supplementary Fig. 5). Most strikingly, the majority of APs are emitted during the 10–20 ms after the stimulus, and most of these were emitted by L5 thick-tufted cells. In summary, a single deflection of the PW, which is anatomically and functionally represented by ∼8500 excitatory cells in the PW cortical column, generates ∼4000 APs.

Discussion

The results suggest that the major AP output of a cortical column, both during spontaneous activity and in response to a simple whisker deflection, is generated by thick-tufted cells located in L5. More specifically, after a sensory stimulus 60% of all evoked APs in the main output layers (L2/3 and L5) are generated by L5 thick-tufted cells. The APs emitted by layer 2/3 cells and L5 slender-tufted cells account for only a small fraction of the total columnar AP output (25 and 15%, respectively). Thus stimulus representation in the barrel cortex is layer-specific but in L5 also highly cell-type-specific, since L5 slender-tufted and L5 thick-tufted cells differ in almost all properties we investigated. For all cortical layers from which we recorded APs (L2/3, L4, L5 and L6), the average response amplitude per cell was low (< 1 AP per stimulus). Additionally, a whisker deflection activated only a small fraction of the cells constituting a column. This is referred to as 'sparse coding' and has been suggested as a general coding mechanism for visual, auditory and motor cortex (Vinje & Gallant, 2000; DeWeese *et al.* 2003; Brecht *et al.* 2004; Olshausen & Field, 2004).

Spontaneous output

The pattern of APs that we describe in the different layers directly reflects the input they provide to their

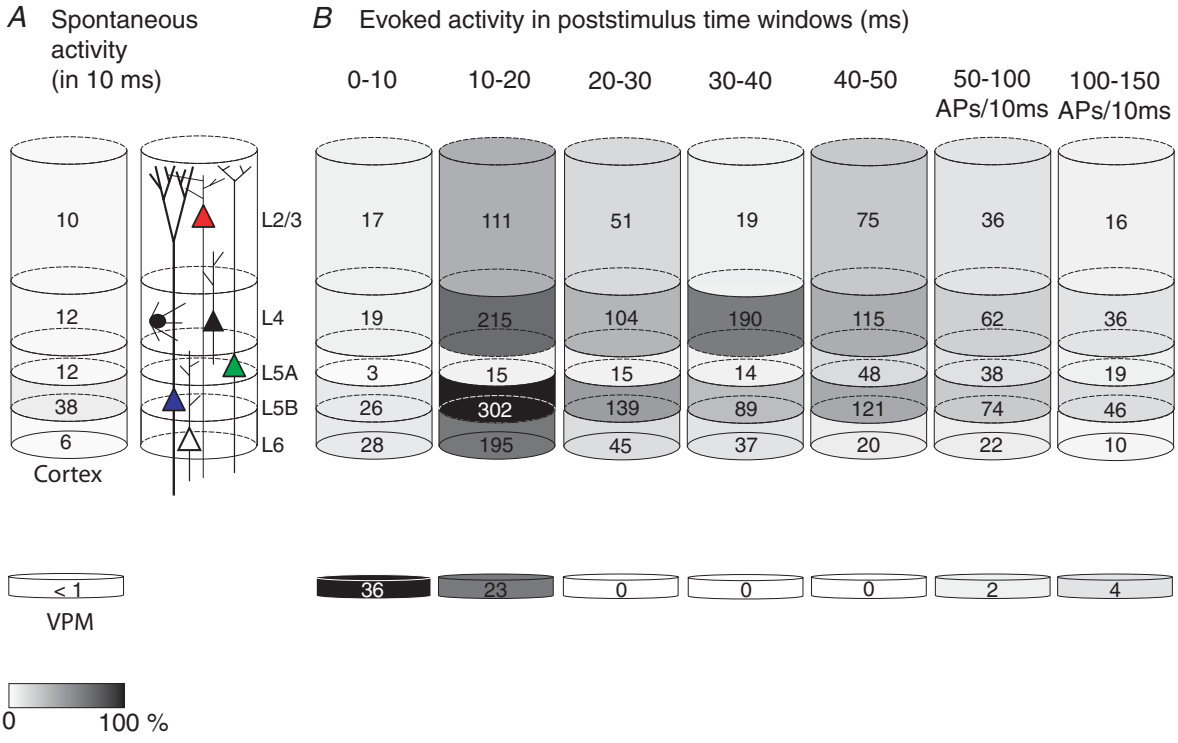

Figure 8. Schematic representation of APs emitted across different layers in barrel cortex column after PW deflection
Number of APs per cell was multiplied by the number of cells present in the column (see Results) to calculate the total number of APs generated by each layer. Values are represented in grey values and normalized to peak activity (maximum number of APs per layer and time frame; here L5 thick-tufted cells at 10–20 ms). *A*, spontaneous APs. *B*, evoked APs. Note that the bulk of evoked APs is in the 10–20 ms window post-stimulus and that most APs are generated by L5 thick-tufted cells.

target structures. In comparison to L2/3 cells, the stream of APs emitted spontaneously from the thick-tufted cells in L5B is substantial. The ensemble of thick-tufted cells of a single column emits about 3800 APs s^{-1} to their target structures, such as thalamus and the motor nuclei in the brainstem connecting to the cerebellum. The relatively high spontaneous rate of APs emitted by L5 thick-tufted cells could generate a persisting tonic depolarization of the target cell dendrites. For example, the thalamocortical–paralemniscal projection (via L5B–POm–L5A connections) could be substantially modulated via the spontaneous output of L5 thick-tufted cells to the POm (Hoogland *et al.* 1991; Diamond *et al.* 1992*a*). In turn, spontaneous APs emitted by L5A cells could, because of L5A-to-L1 axonal projections, continuously depolarize the apical tuft dendrites of cortical pyramidal cells, thereby favouring the generation of bursts of APs (Larkum & Zhu, 2002; Larsen & Callaway, 2006). The large difference of spontaneous APs observed in different layers is, with respect to underlying mechanisms, unclear. However, the low spontaneous activity in thalamus under anaesthesia (Bruno & Sakmann, 2006) suggests a cortical rather than a thalamic origin.

Evoked output

The L5 thick-tufted cells also dominate the evoked output of the cortical column. The peak of AP activity is during the interval of 10–20 ms after the sensory stimulus and returns to baseline within 150 ms (which is true for all cell types), which corresponds to the time window between consecutive whisking movements (e.g. at 7–12 Hz). Furthermore, the receptive field (RF) of L5 thick-tufted cells is not only restricted to principal whisker (PW) responses but L5 thick-tufted cells also collect sensory information from neighbouring whiskers (Fig. 6; see also Ito, 1992). This is in contrast to the other cell types and layers, where RFs are primarily restricted to PW responses. The target areas of L5 thick-tufted cells are thalamus and the motor nuclei in the brainstem connecting to the cerebellum (Jenkinson & Glickstein, 2000; Leergaard *et al.* 2000; Killackey & Sherman, 2003). Whisker movements activate the cerebellum in a very precise fashion (Chadderton *et al.* 2004), suggesting that cerebellar activity and consequently motor reactions are controlled by L5 thick-tufted cells. The VPM–L5B projection may provide a fast 'bypass' to direct the animals' behaviour initially.

Simultaneous representation in multiple layers

After a sensory stimulus, we observed APs almost simultaneously in L4, L5 thick-tufted cells and L6 and occasionally in L2/3 cells (Fig. 4*A*). These observations directly argue against the hypothesis that electrical activity always begins in L4, from where it spreads throughout the column to sequentially activate the other layers in a hierarchical order (Li *et al.* 1956; Simons, 1978; Armstrong-James *et al.* 1992; Moore & Nelson, 1998; Douglas & Martin, 2004; Wilent & Contreras, 2004). It is more likely that simultaneous AP activity in these layers results, at least during the initial 10–20 ms after a sensory stimulus, from excitation via VPM afferents, which is then followed by sequential activation by intracolumnar radial projections from L4 cells (Mountcastle, 1957; Johnson & Alloway, 1995; Laaris *et al.* 2000; Ahissar *et al.* 2001). However, net excitation provided by VPM and L4 inputs varies between different layers. Specifically, the APs evoked in L4, L5 thick-tufted cells and L6 are likely to be activated initially by synaptic input from VPM. This view is based on onset latency measurements of EPSPs, which (except for L2) varies only between 8 and 10 ms for L4, L5B and L6 (Carvell & Simons, 1988; Moore & Nelson, 1998; Brecht & Sakmann, 2002*b*; Brecht *et al.* 2003; Manns *et al.* 2004). Thus the peak of AP activity in L5B and L6 is unlikely to be due to polysynaptic input via L4. On average, APs in L6 cells even seem to precede APs in L4, perhaps owing to differences in excitability, release probability and quantal content of VPM–L6 synapses, and/or weaker feedforward inhibition. Thus early AP activity in this layer cannot be explained by excitatory input from L4. The observation that AP peaks in L2/3 and L5A are delayed with respect to the peaks in L4, L5 thick-tufted cells and L6 could either result from delayed activation of the paralemniscal pathway (Diamond *et al.* 1992*b*; Ahissar *et al.* 2000; Sosnik *et al.* 2001) or could mean that in these layers sequential input from L4 is more important for spiking (Brecht *et al.* 2003; Feldmeyer *et al.* 2005; Schubert *et al.* 2006). Compound EPSPs evoked in L2/3 cells in fact have several components (Brecht *et al.* 2003), which could reflect input from both VPM and L4. Since the contributions of these components depend on stimulus intensity (M. Brecht & B. Sakmann, unpublished observations), the relative impact of VPM and L4 input on the AP output of a particular cell type may well change with stimulus intensity.

Classification of cell types

In L5, we characterized two cell types, based on the diameter of cell body, diameter of apical dendrite and branching pattern of apical tuft. Accordingly, we separated L5 cells into slender- and thick-tufted pyramids and found major differences in spontaneous activity, evoked activity, latency and receptive field size. Surprisingly, most of these differences were not observed in whole-cell recordings (Manns *et al.* 2004). One explanation could be that whole-cell dialysis affects AP spiking, but a more likely explanation is the use of different classifications. In our tangential sections, it is not possible to define the L5A–L5B border and therefore we classified cells as L5 slender-tufted and L5 thick-tufted cells. In the previous study (Manns

et al. 2004), cells were categorized as L5A and L5B cells using (semi)coronal sections, in which the border is clear. In our classification, L5 slender- and L5 thick-tufted cells are most likely to be representative for L5A and L5B, since L5 slender-tufted cells are activated with long latency and L5 thick-tufted cells with short latency (Ahissar *et al.* 2000). However, L5 slender-tufted cells can also be located in L5B (Schubert *et al.* 2001) and can therefore lead to different results, depending on the classification method.

Cell-type-specific sensory representation

We showed that in L5, representation of the sensory stimulus is cell-type-specific. In contrast, in L4 and L6 we did not find obvious differences in response properties between morphologically different classifications. It was recently suggested that in L4, cell-type-specific circuits may coexist that represent the stimulus similarly but serve different functions (Staiger *et al.* 2004). More specifically, spiny stellates would relay sensory information exclusively within the column by means of their almost exclusively columnar axonal arbors, whereas pyramidal neurones are involved in transcolumnar processing via horizontal collaterals (Staiger *et al.* 2004). In L6, a similar corepresentation could occur that could allow sensory coprocessing in morphologically distinct (e.g. cortico-thalamic and corticocortical) networks.

Response variability

In sensory cortices, repeated stimuli evoke responses that vary from trial to trial (Arieli *et al.* 1996; Amarasingham *et al.* 2006; Gur & Snodderly, 2006; but see DeWeese *et al.* 2003, 2005). In our experiments, sensory-evoked responses were also not stereotyped and response variability was, in addition, cell-type- and layer-specific. The lowest trial-to-trial variability in cortex was observed in L4 cells, L5 thick-tufted cells and a subset of L6 cells, and was comparable to the response variability of VPM cells, known to innervate these three particular regions. In contrast, L2/3 cells and L5 slender-tufted cells showed AP responses that were much lower and had a higher trial-to-trial variability. On-going network activity (Arieli *et al.* 1996), segregated sensory input (Koralek *et al.* 1988) and intrinsic properties (Ito & Kato, 2002) could underlie the observed response variability. Comparison of averaged responses from individual cells revealed that responses of L5 thick-tufted cells were highly comparable with each other. In contrast, cell-to-cell comparisons for other cell types showed much less similarity. In summary, L5 thick-tufted cells have the lowest trial-to-trial variability and cell-to-cell variability, which may imply that these cells most reliably convey sensory information to other brain areas.

Effect of anaesthesia

We observed low response amplitudes after sensory stimuli for all cortical layers. Although spiking frequencies could be significantly depressed by urethane anaesthesia, L2/3 cells have comparable levels of AP discharges under awake conditions (Crochet & Petersen, 2006). In addition, in somatosensory cortex, urethane was shown only to affect the response latency to deflection of SuWs. For PW deflection, both the amplitude and the response latency were not significantly different for awake and urethane conditions (Simons *et al.* 1992). We argue that the magnitudes of our responses obtained under urethane anaesthesia are not necessarily different from those obtained under awake conditions.

Output of the cortical column

In conclusion, we can now estimate the total number of APs that are emitted in the barrel cortex after a whisker deflection that could drive the behavioural response. The ensemble of about 9000 L5 thick-tufted cells in the PW and all eight first order SuW columns emit ∼4000 APs after a single whisker deflection. In contrast, the ensemble of 29 000 L2/3 and 10 000 L5 slender-tufted cells emit only ∼1275 and ∼600 APs, respectively. Layer 5 thick-tufted cells thus dominate the AP output of the cortical column, which could imply that this cell type guides sensory-evoked behaviour. Here we demonstrated the cell-type-specific properties for excitatory cells. Equally important is the question of whether inhibitory neurones have layer-specific responses as well, and how inhibitory neurones contribute to the cell- and layer-specificity we have described. In addition, experiments on awake animals will be necessary to elucidate the different involvement of cortical layers in more complex behaviours (Celikel & Sakmann, 2007) to validate whether the layer-specific AP distributions that we observe in anaesthetized animals are comparable in the cortex of awake animals.

References

Agmon A & Connors BW (1992). Correlation between intrinsic firing patterns and thalamocortical synaptic responses of neurons in mouse barrel cortex. *J Neurosci* **12**, 319–329.

Agmon A, Yang LT, O'Dowd DK & Jones EG (1993). Organized growth of thalamocortical axons from the deep tier of terminations into layer IV of developing mouse barrel cortex. *J Neurosci* **13**, 5365–5382.

Ahissar E, Sosnik R, Bagdasarian K & Haidarliu S (2001). Temporal frequency of whisker movement. *II. Laminar organization of cortical representations. J Neurophysiol* **86**, 354–367.

Ahissar E, Sosnik R & Haidarliu S (2000). Transformation from temporal to rate coding in a somatosensory thalamocortical pathway. *Nature* **406**, 302–306.

Alloway KD, Crist J, Mutic JJ & Roy SA (1999). Corticostriatal projections from rat barrel cortex have an anisotropic organization that correlates with vibrissal whisking behavior. *J Neurosci* **19**, 10908–10922.

Amarasingham A, Chen TL, Geman S, Harrison MT & Sheinberg DL (2006). Spike count reliability and the Poisson hypothesis. *J Neurosci* **26**, 801–809.

Arieli A, Sterkin A, Grinvald A & Aertsen A (1996). Dynamics of ongoing activity: explanation of the large variability in evoked cortical responses. *Science* **273**, 1868–1871.

Armstrong-James M, Fox K & Das-Gupta A (1992). Flow of excitation within rat barrel cortex on striking a single vibrissa. *J Neurophysiol* **68**, 1345–1358.

Beaulieu C (1993). Numerical data on neocortical neurons in adult rat, with special reference to the GABA population. *Brain Res* **609**, 284–292.

Brecht M, Roth A & Sakmann B (2003). Dynamic receptive fields of reconstructed pyramidal cells in layers 3 and 2 of rat somatosensory barrel cortex. *J Physiol* **553**, 243–265.

Brecht M & Sakmann B (2002*a*). Whisker maps of neuronal subclasses of the rat ventral posterior medial thalamus, identified by whole-cell voltage recording and morphological reconstruction. *J Physiol* **538**, 495–515.

Brecht M & Sakmann B (2002*b*). Dynamic representation of whisker deflection by synaptic potentials in spiny stellate and pyramidal cells in the barrels and septa of layer 4 rat somatosensory cortex. *J Physiol* **543**, 49–70.

Brecht M, Schneider M, Sakmann B & Margrie TW (2004). Whisker movements evoked by stimulation of single pyramidal cells in rat motor cortex. *Nature* **427**, 704–710.

Bruno RM, Khatri V, Land PW & Simons DJ (2003). Thalamocortical angular tuning domains within individual barrels of rat somatosensory cortex. *J Neurosci* **23**, 9565–9574.

Bruno RM & Sakmann B (2006). Cortex is driven by weak but synchronously active thalamocortical synapses. *Science* **312**, 1622–1627.

Carvell GE & Simons DJ (1988). Membrane potential changes in rat SmI cortical neurons evoked by controlled stimulation of mystacial vibrissae. *Brain Res* **448**, 186–191.

Carvell GE & Simons DJ (1995). Task- and subject-related differences in sensorimotor behavior during active touch. *Somatosens Mot Res* **12**, 1–9.

Celikel T & Sakmann B (2007). Sensory intergration across space and in time for decision making in the somatosensory system of rodents. *Proc Natl Acad Sci U S A* **104**, 1395–1400.

Chadderton P, Margrie TW & Hausser M (2004). Integration of quanta in cerebellar granule cells during sensory processing. *Nature* **428**, 856–860.

Chagnac-Amitai Y, Luhmann HJ & Prince DA (1990). Burst generating and regular spiking layer 5 pyramidal neurons of rat neocortex have different morphological features. *J Comp Neurol* **296**, 598–613.

Chmielowska J, Carvell GE & Simons DJ (1989). Spatial organization of thalamocortical and corticothalamic projection systems in the rat SmI barrel cortex. *J Comp Neurol* **285**, 325–338.

Crochet S & Petersen CC (2006). Correlating whisker behavior with membrane potential in barrel cortex of awake mice. *Nat Neurosci* **9**, 608–610.

DeWeese MR, Hromadka T & Zador AM (2005). Reliability and representational bandwidth in the auditory cortex. *Neuron* **48**, 479–488.

DeWeese MR, Wehr M & Zador AM (2003). Binary spiking in auditory cortex. *J Neurosci* **23**, 7940–7949.

Diamond ME, Armstrong-James M, Budway MJ & Ebner FF (1992*a*). Somatic sensory responses in the rostral sector of the posterior group (POm) and in the ventral posterior medial nucleus (VPM) of the rat thalamus: dependence on the barrel field cortex. *J Comp Neurol* **319**, 66–84.

Diamond ME, Armstrong-James M & Ebner FF (1992*b*). Somatic sensory responses in the rostral sector of the posterior group (POm) and in the ventral posterior medial nucleus (VPM) of the rat thalamus. *J Comp Neurol* **318**, 462–476.

Douglas RJ & Martin KA (2004). Neuronal circuits of the neocortex. *Annu Rev Neurosci* **27**, 419–451.

Feldmeyer D, Roth A & Sakmann B (2005). Monosynaptic connections between pairs of spiny stellate cells in layer 4 and pyramidal cells in layer 5A indicate that lemniscal and paralemniscal afferent pathways converge in the infragranular somatosensory cortex. *J Neurosci* **25**, 3423–3431.

Gur M & Snodderly DM (2006). High response reliability of neurons in primary visual cortex (V1) of alert, trained monkeys. *Cereb Cortex* **16**, 888–895.

Hoffer ZS, Arantes HB, Roth RL & Alloway KD (2005). Functional circuits mediating sensorimotor integration: quantitative comparisons of projections from rodent barrel cortex to primary motor cortex, neostriatum, superior colliculus, and the pons. *J Comp Neurol* **488**, 82–100.

Hoogland PV, Wouterlood FG, Welker E & Van der Loos H (1991). Ultrastructure of giant and small thalamic terminals of cortical origin: a study of the projections from the barrel cortex in mice using *Phaseolus vulgaris* leuco-agglutinin (PHA-L). *Exp Brain Res* **87**, 159–172.

Hoover JE, Hoffer ZS & Alloway KD (2003). Projections from primary somatosensory cortex to the neostriatum: the role of somatotopic continuity in corticostriatal convergence. *J Neurophysiol* **89**, 1576–1587.

Horikawa K & Armstrong WE (1988). A versatile means of intracellular labeling: injection of biocytin and its detection with avidin conjugates. *J Neurosci Methods* **25**, 1–11.

Hutson KA & Masterton RB (1986). The sensory contribution of a single vibrissa's cortical barrel. *J Neurophysiol* **56**, 1196–1223.

Ito M (1992). Simultaneous visualization of cortical barrels and horseradish peroxidase-injected layer 5b vibrissa neurones in the rat. *J Physiol* **454**, 247–265.

Ito M & Kato M (2002). Analysis of variance study of the rat cortical layer 4 barrel and layer 5b neurones. *J Physiol* **539**, 511–522.

Jenkinson EW & Glickstein M (2000). Whiskers, barrels, and cortical efferent pathways in gap crossing by rats. *J Neurophysiol* **84**, 1781–1789.

Johnson MJ & Alloway KD (1995). Evidence for synchronous activation of neurons located in different layers of primary somatosensory cortex. *Somatosens Mot Res* **12**, 235–247.

Killackey HP & Sherman SM (2003). Corticothalamic projections from the rat primary somatosensory cortex. *J Neurosci* **23**, 7381–7384.

Kim U & Ebner FF (1999). Barrels and septa: separate circuits in rat barrels field cortex. *J Comp Neurol* **408**, 489–505.

Koralek KA, Jensen KF & Killackey HP (1988). Evidence for two complementary patterns of thalamic input to the rat somatosensory cortex. *Brain Res* **463**, 346–351.

Laaris N, Carlson GC & Keller A (2000). Thalamic-evoked synaptic interactions in barrel cortex revealed by optical imaging. *J Neurosci* **20**, 1529–1537.

Larkum ME & Zhu JJ (2002). Signaling of layer 1 and whisker-evoked Ca^{2+} and Na^{+} action potentials in distal and terminal dendrites of rat neocortical pyramidal neurons *in vitro* and *in vivo*. *J Neurosci* **22**, 6991–7005.

Larsen DD & Callaway EM (2006). Development of layer-specific axonal arborizations in mouse primary somatosensory cortex. *J Comp Neurol* **494**, 398–414.

Leergaard TB, Lyngstad KA, Thompson JH, Taeymans S, Vos BP, De Schutter E, Bower JM & Bjaalie JG (2000). Rat somatosensory cerebropontocerebellar pathways: spatial relationships of the somatotopic map of the primary somatosensory cortex are preserved in a three-dimensional clustered pontine map. *J Comp Neurol* **422**, 246–266.

Li CL, Cullen C & Jasper HH (1956). Laminar microelectrode studies of specific somatosensory cortical potentials. *J Neurophysiol* **19**, 111–130.

Lu SM & Lin RC (1993). Thalamic afferents of the rat barrel cortex: a light- and electron-microscopic study using *Phaseolus vulgaris* leucoagglutinin as an anterograde tracer. *Somatosens Mot Res* **10**, 1–16.

Manns ID, Sakmann B & Brecht M (2004). Sub- and suprathreshold receptive field properties of pyramidal neurones in layers 5A and 5B of rat somatosensory barrel cortex. *J Physiol* **556**, 601–622.

Markram H (1997). A network of tufted layer 5 pyramidal neurons. *Cereb Cortex* **7**, 523–533.

Mason A & Larkman A (1990). Correlations between morphology and electrophysiology of pyramidal neurons in slices of rat visual cortex. *II. Electrophysiology. J Neurosci* **10**, 1415–1428.

Moore CI & Nelson SB (1998). Spatio-temporal subthreshold receptive fields in the vibrissa representation of rat primary somatosensory cortex. *J Neurophysiol* **80**, 2882–2892.

Mountcastle VB (1957). Modality and topographic properties of single neurons of cat's somatic sensory cortex. *J Neurophysiol* **20**, 408–434.

Mountcastle VB (1997). The columnar organization of the neocortex. *Brain* **120**, 701–722.

Olshausen BA & Field DJ (2004). Sparse coding of sensory inputs. *Curr Opin Neurobiol* **14**, 481–487.

Pinault D (1996). A novel single-cell staining procedure performed in vivo under electrophysiological control: morpho-functional features of juxtacellularly labeled thalamic cells and other central neurons with biocytin or Neurobiotin. *J Neurosci Methods* **65**, 113–136.

Schubert D, Kotter R, Luhmann HJ & Staiger JF (2006). Morphology, electrophysiology and functional input connectivity of pyramidal neurons characterizes a genuine layer Va in the primary somatosensory cortex. *Cereb Cortex* **16**, 223–236.

Schubert D, Staiger JF, Cho N, Kotter R, Zilles K & Luhmann HJ (2001). Layer-specific intracolumnar and transcolumnar functional connectivity of layer V pyramidal cells in rat barrel cortex. *J Neurosci* **21**, 3580–3592.

Simons DJ (1978). Response properties of vibrissa units in rat SI somatosensory neocortex. *J Neurophysiol* **41**, 798–820.

Simons DJ, Carvell GE, Hershey AE & Bryant DP (1992). Responses of barrel cortex neurons in awake rats and effects of urethane anesthesia. *Exp Brain Res* **91**, 259–272.

Sosnik R, Haidarliu S & Ahissar E (2001). Temporal frequency of whisker movement. I. Representations in brain stem and thalamus. *J Neurophysiol* **86**, 339–353.

Staiger JF, Flagmeyer I, Schubert D, Zilles K, Kotter R & Luhmann HJ (2004). Functional diversity of layer IV spiny neurons in rat somatosensory cortex: quantitative morphology of electrophysiologically characterized and biocytin labeled cells. *Cereb Cortex* **14**, 690–701.

Varga C, Sik A, Lavallee P & Deschenes M (2002). Dendroarchitecture of relay cells in thalamic barreloids: a substrate for cross-whisker modulation. *J Neurosci* **22**, 6186–6194.

Vinje WE & Gallant JL (2000). Sparse coding and decorrelation in primary visual cortex during natural vision. *Science* **287**, 1273–1276.

Wilent WB & Contreras D (2004). Synaptic responses to whisker deflections in rat barrel cortex as a function of cortical layer and stimulus intensity. *J Neurosci* **24**, 3985–3998.

Wise SP & Jones EG (1977). Cells of origin and terminal distribution of descending projections of the rat somatic sensory cortex. *J Comp Neurol* **175**, 129–157.

Wong-Riley M (1979). Changes in the visual system of monocularly sutured or enucleated cats demonstrable with cytochrome oxidase histochemistry. *Brain Res* **171**, 11–28.

Woolsey TA & Van der Loos H (1970). The structural organization of layer IV in the somatosensory region (SI) of mouse cerebral cortex. The description of a cortical field composed of discrete cytoarchitectonic units. *Brain Res* **17**, 205–242.

Zhang ZW & Deschenes M (1997). Intracortical axonal projections of lamina VI cells of the primary somatosensory cortex in the rat: a single-cell labeling study. *J Neurosci* **17**, 6365–6379.

Acknowledgements

This work was supported by the Max-Planck Society. We thank Tansu Celikel and Rainer Friedrich for comments on previous versions of the manuscript, Marlies Kaiser and Ellen Stier for histology, Rolf Rödel and Karl Schmidt for technical assistance and Sebastiano Bellanca, Thomas Mock and Andrea Weber for Neurolucida reconstructions.

Supplemental material

Online supplemental material for this paper can be accessed at:
http://jp.physoc.org/cgi/content/full/jphysiol.2006.124321/DC1
and
http://www.blackwell-synergy.com/doi/suppl/10.1113/jphysiol.2006.124321